ACS Sustainable Chemistry & Engineering

Research Article

Cite This: ACS Sustainable Chem. Eng. 2020, 8, 1276−1284

pubs.acs.org/journal/ascecg

Photoinduced Upgrading of Lactic Acid-Based Solvents to Block Copolymer Surfactants

Nabil Bensabeh,[†,⊥] Adrian Moreno,[†,⊥] Adrià Roig,[†] Mehrnoush Rahimzadeh,[‡,§] Khosrow Rahimi,[‡,§] Juan Carlos Ronda,[†] Virginia Cádiz,[†] Marina Galià,[†] Virgil Percec,*[,∥] Cesar Rodriguez-Emmenegger,*[,‡,§] and Gerard Lligadas*[,†,∥]

[†]Laboratory of Sustainable Polymers, Department of Analytical Chemistry and Organic Chemistry, University Rovira i Virgili, C/ Marcel.lí Domingo 1, 43007 Tarragona, Spain

[‡]DWI-Leibniz Institute for Interactive Materials, Forckenbeckstraße 50, 52074 Aachen, Germany

[§]Institute of Technical and Macromolecular Chemistry, RWTH Aachen University, Worringerweg 1-2, 52074 Aachen, Germany

[∥]Roy & Diana Vagelos Laboratories, Department of Chemistry, University of Pennsylvania, 231 S. 34th Street, Philadelphia, Pennsylvania 19104-6323, United States

Supporting Information

ABSTRACT: We report a new strategy toward the development of block copolymer surfactants from chemicals of the lactic acid family. A particularly unique aspect of this work is the use of green solvents as biobased platform chemicals to generate well-defined and nanostructure-forming materials. Herein, efficient functionalization of ethyl lactate (EL) and *N*,*N*-dimethyl lactamide (DML) solvents with acrylate groups generated monomers that could be polymerized by the photoinduced copper-catalyzed living radical polymerization process to yield polymeric materials with different water solubilities. These lactic acid-derived monomers were used as a major component in well-defined diblock copolymers composed of poly(EL acrylate) and poly(DML acrylate) segments as hydrophobic and hydrophilic building blocks, respectively. The resulting amphiphilic copolymers could self-assemble in aqueous solution to form nanoparticles with different morphologies (e.g., large-compound micelles and vesicles). Subsequently, the formed amphiphilic polymers were employed as efficient stabilizers in the emulsion polymerization of methyl methacrylate and styrene, offering a facile method for the synthesis of well-defined and stable polymer latexes in the range of 100−200 nm, demonstrating the practical significance of these biobased polymers in nanomaterial synthesis.

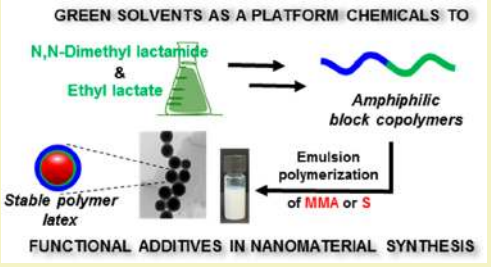

KEYWORDS: *green solvent, sustainable copolymers, amphiphilic, photopolymerization, living radical polymerization, emulsion polymerization*

INTRODUCTION

Biomass-derived platform chemicals are gaining momentum in both industry and academia because of dwindling of fossil fuel resources and environmental concerns.[1−4] In this regard, lactic acid is one of the top feedstock given its ready availability from renewable carbohydrates via fermentation or chemocatalytic routes,[5,6] and its facile conversion into a number of important derivatives such as fine and commodity chemicals, biodegradable polymers, and fuel precursors.[7−10] Among them, ethyl lactate (EL)[11] and *N*,*N*-dimethyl lactamide (DML)[12] are in the portfolio of available green biosolvents suitable to replace traditional chemicals because they offer an appealing combination of properties including high boiling point, high solvency power, negligible toxicity, and 100% biodegradability that translate into important environmental benefits and performance advantages.[13−16] The use of EL, for example, enabled to improve the green angle of numerous organic transformations such as olefin metathesis[17] and cycloaddition[18] reactions. The instability of Cu(I)X/N−ligand complexes toward disproportionation in DML[19] and EL[20] also facilitated their application as efficient green reaction media in Cu(0)-mediated SET-LRP reactions.[21,22] However, the potential of these simple and cheap lactic acid deriavatives[23] goes beyond their academic use as they have been used in many industrial applications including the preparation of agrochemical[24] and cleaning formulations,[25] polymeric membranes in a safe workplace,[26] among others.[13,27−29]

The chemical structure of EL and DML is also of great appeal to expand the scope of potential application of these green solvents as sustainable feedstock for sustainable polymer synthesis.[30−32] Their secondary alcohol offers a simple access to monovinyl derivatives for use in either free or living radical chain growth polymerizations (FRP and LRP, respectively). In this regard, a few publications reported that acrylic and

Received: November 5, 2019
Revised: December 5, 2019
Published: December 11, 2019

DOI: 10.1021/acssuschemeng.9b06599
ACS Sustainable Chem. Eng. 2020, 8, 1276−1284

Scheme 1. Synthesis of ELA and DMLA Monomers from the Corresponding Green Solvents and Subsequent Cu(II)-Mediated Radical Photopolymerization[a]

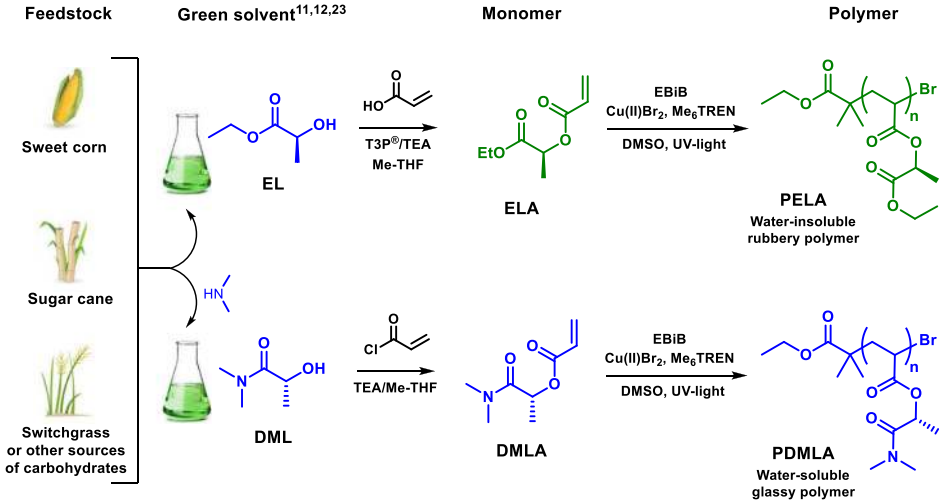

[a]Color code: blue, hydrophilic and water-soluble and green, hydrophobic and water-insoluble.

methacrylic derivatives of lactic acid esters (i.e., methyl, ethyl, butyl) are suitable to polymerize by FRP to yield water-insoluble rubbery polymers.[33−36] More recently, our group also reported that well-defined polymers derived from this toolbox of monomers are easily accessible by Cu(0) wire-mediated SET-LRP.[37,38] However, vinylic derivatives of *N*-alkyl lactamides and polymers thereof are only reported in the old patent literature,[39] and no study on their physical properties, LRP as well as block copolymer (BCP) synthesis, is yet available to the best of our knowledge.

Herein, we sought to enable the development of advanced materials such as BCPs[40−42] using EL and DML green solvents as biobased platform molecules by synthesizing and polymerizing the corresponding acrylic derivatives. The different water solubility demonstrated by the corresponding homopolymers, that is, poly(EL acrylate) (PELA) is hydrophobic and water-insoluble and poly(DML acrylate) (PDMLA) is hydrophilic and water-soluble, drove our interest to study the overall ability of the resulting sustainable BCPs to undergo self-assembly under aqueous conditions. The innovative sustainable amphiphilic copolymers reported in this study showed promise as polymeric surfactants in the aqueous emulsion polymerization of commodity monomers such as methyl methacrylate (MMA) and styrene (S).

EXPERIMENTAL SECTION

General Procedure for the in Situ Cu(II)-Mediated Radical Block Photocopolymerization of ELA and DMLA. The procedure is generic for all the BCPs prepared herein. The block copolymerization of ELA ($[ELA]_0/[EBiB]_0/[Cu(II)Br_2]_0/[Me_6TREN]_0$ = 50/1/0.02/0.12) with DMLA (50 equiv) is described. ELA (0.5 mL, 3.11 mmol) and Me_6TREN (2 μL, 0.0075 mmol) were added in a vial containing a small Teflon-coated stirring bar. Afterwards, 0.5 mL of stock solution containing ethyl α-bromoisobutyrate (EBiB) (36.6 μL, 0.062 mmol) and $Cu(II)Br_2$ (1.12 mg, 0.0013 mmol) in dimethyl sulfoxide (DMSO) was introduced to the reaction mixture. After sealing the flask with a rubber septum and bubbling argon through the reaction mixture for 15 min, the vial was placed under UV light irradiation while stirring. After 2.5 h, the reaction mixture was sampled using an airtight syringe under positive pressure of argon to determine ELA conversion by ^1H NMR spectroscopy. After that, a solution DMLA (0.44 mL, 3.11 mmol) and Me_6TREN (2 μL, 0.0075 mmol) in DMSO (0.44 mL), previously deoxygenated was injected into the polymerization mixture via a cannula. The reaction mixture was placed again under UV light and allowed to proceed for additional 2.5 h. Finally, the DMLA conversion was determined by ^1H NMR spectroscopy and M_n and M_w/M_n values by gel permeation chromatography (GPC) using PMMA standards. The obtained copolymer was purified through dialysis against acetone and dried under vacuum until constant weight. The critical aggregation concentration (CAC) of selected copolymers was determined by using Nile Red (NR) as a fluorescence probe by monitoring the emission peaks at 585 nm. A copolymer concentration ranging from 1.0×10^{-9} to 1.0 $g \cdot L^{-1}$ was used. The NR concentration was fixed at 6.0×10^{-7} M.

Self-Assembly of BCPs. BCP1 nanoassemblies were prepared by direct dissolution of 0.5 mg of copolymer in 10 mL of Milli-Q water. BCP2 nanoassemblies were prepared by two different methods: (i) fast injection of a solution of copolymer in THF (5 $mg \cdot mL^{-1}$) to milli Q water at room temperature and (ii) fast injection of the same solution to milli Q water at 80 °C.

RESULTS AND DISCUSSION

Synthesis of ELA and DMLA. As reported in a previous publication,[37] EL solvent was used as a biobased platform chemical to synthesize its acrylic derivative (ELA, Scheme 1). ELA was synthesized using an environmentally friendly approach using acrylic acid as a main reagent and T3P as an ester-coupling promoter in the presence of TEA.[43] To maximize the green angle of the process, a solvent with low environmental impact such as Me-THF was used. After a simple work-up method with no chromatographic purification, ELA was obtained in 52% yield. Unfortunately, although research to improve this procedure continues to be in progress, at this time this attractive procedure was not employed to install the acrylate functionality on the DML solvent (vide infra). Therefore, the acylation of DML with acryloyl chloride in the presence of TEA afforded the corresponding optically active ($[\alpha]_D^{25}$ = +8.0, *c* 1.0 mg/mL, MeCN) acrylic ester-amide monomer (DMLA) as a colorless liquid after vacuum distillation (70% yield). Although EL solvent is miscible in water and common organic solvents, the corresponding acrylic derivative (ELA) turned insoluble in water. However, switching the ethyl ester moiety to an *N*,*N*-dimethyl substituted

DOI: 10.1021/acssuschemeng.9b06599
ACS Sustainable Chem. Eng. 2020, 8, 1276−1284

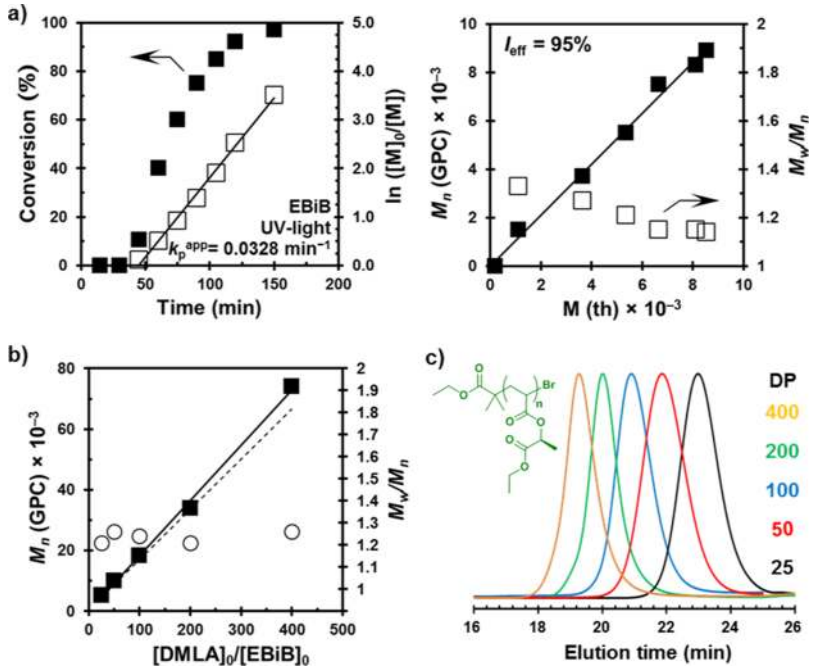

Figure 1. (a) Kinetics plots and evolution of experimental M_n (GPC) and M_w/M_n vs theoretical M_n^{th} for the Cu(II)-mediated living photopolymerization of DMLA in DMSO. Reaction conditions: $[DMLA]_0/[EBiB]_0/[Me_6\text{-TREN}]_0/[Cu(II)Br_2]_0$ = 50/1/0.12/0.02. (b) Dependence of experimental M_n (GPC) and M_w/M_n on $[DMLA]_0/[EBiB]_0$ ratio for the photopolymerization of DMLA in DMSO. (c) GPC traces (normalized to peak height) of PELA with different targeted DPs (25−400).

amide resulted in a water-soluble vinylic monomer (DMLA) that, as will be discussed lately, enabled us to prepare new amphiphilic BCPs from these two lactic acid-derived monomers. Unfortunately, the water solubility of DMLA compromised the isolation of this monomer after synthesis via T3P-promoted esterification with acrylic acid.

The structure of both monomers was verified by NMR and high-resolution mass spectrometry (Figures S1−S4). Previously, our group and others demonstrated that ELA is prone to polymerize either by FRP or LRP to deliver water-insoluble rubbery polymers (i.e., PELA).[33−37] The ability of DMLA to polymerize by FRP using AIBN as the initiator was confirmed by ^{1}H NMR and GPC. ^{1}H NMR analysis indicated 96% monomer conversion after 8 h at 90 °C. The resulting polymer, named thereafter PDMLA, was soluble at 10 wt % in polar organic solvents such as THF, CH_2Cl_2, $CHCl_3$, acetone, and DMF but also in water. This hydrophilic polymer could also be dissolved in DML and EL. Compared to ^{1}H NMR spectrum of the monomeric precursor, the ^{1}H NMR spectrum of PDMLA recorded in D_2O revealed the successful formation of the saturated polymer backbone by the absence of the olefinic protons and the appearance of the characteristic signals at 1.35−2.65 ppm corresponding to the polymer backbone (Figure S5). GPC analysis in DMF (0.1 wt % LiBr) was used to determine number-average molar mass (M_n) = 27 300 g mol^{-1} and molecular weight distribution (M_w/M_n) = 2.9 (Figure S6). Next, the thermal properties of PDMLA were investigated by differential scanning calorimetry (DSC) and thermogravimetric analysis (TGA) techniques. The only thermal event that was detected in the DSC curve was an endothermal baseline shift, associated with the glass transition temperature (T_g), at a remarkably high temperature (75 °C), which is in accordance with the solid appearance of the polymer at room temperature (Figure S7). The T_g of this amorphous polymer is significantly higher than that previously reported for PELA prepared by FRP (T_g = −27 °C).[33] It is believed that polar *N*,*N*-dimethyl amide side groups lead to stronger intermolecular attractive interactions between chains which hinder molecular motion, thus causing an increase in T_g. TGA analysis revealed that after an initial weight loss, associated with some humidity absorbed, the thermal degradation of PDMLA side groups and backbone has a well-defined one-step degradation profile with a maxima at 353 °C (Figure S8).

Photoinduced LRP of DMLA and ELA. Considering the potential of photopolymerization techniques for green and sustainable polymerization processes, the living photopolymerization of DMLA and ELA was investigated. To provide an effective route for the synthesis of well-defined polymers, copper-catalyzed photoinduced radical polymerization was employed in this study.[44−49] Initially, the polymerization of DMLA was performed at ambient temperature using catalytic $Cu(II)Br_2$ (2 mol % with respect to the initiator) and an aliphatic amine ligand, Me_6-TREN, in the presence of UV light ($\lambda_{max} \approx 365$ nm) (Scheme 1). The polymerization of DMLA was initiated from EBiB acting as a monofunctional initiator. When the degree of polymerization (DP) was targeted at 50 using DMSO as a nontoxic green solvent,[50] ^{1}H NMR analysis revealed near quantitative conversion after 3 h according to the disappearance of the vinyl signals between 5.8 and 6.4 ppm (Figure S9). Molecular weight analysis of the resulting polymer by GPC revealed a symmetrical monomodal peak (M_w/M_n = 1.26) (Figure S10). Moreover, the experimental number average molecular weight of the polymer (M_n^{GPC} = 10 000 g·mol^{-1}) determined using PMMA standards was in good agreement with the theoretical value (M_n^{th} = 8800 g·mol^{-1}) calculated from the monomer/initiator ratio and the monomer conversion. Note that the photopolymerization of DMLA in its solvent precursor (i.e., DML) also reached high monomer

DOI: 10.1021/acssuschemeng.9b06599
ACS Sustainable Chem. Eng. 2020, 8, 1276−1284

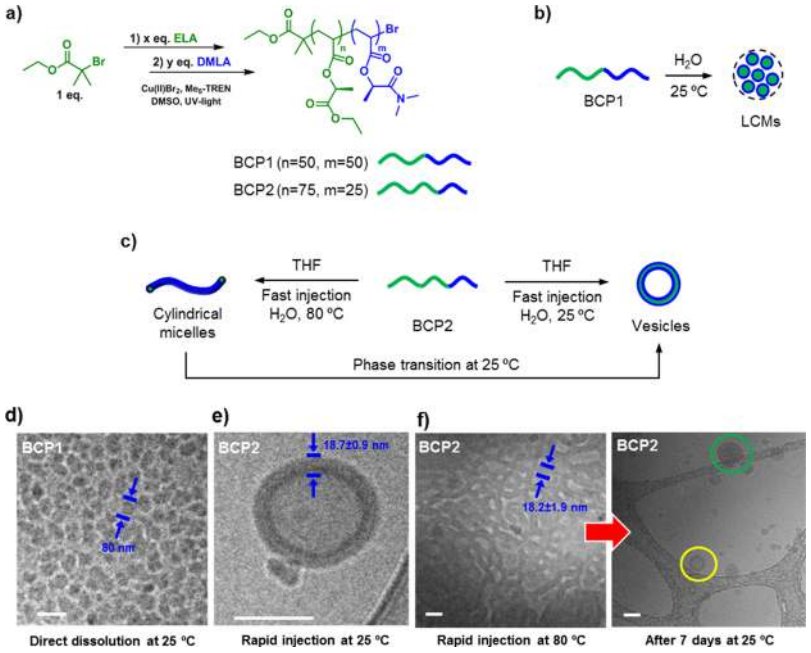

Figure 2. Schematic representations for: (a) synthesis of amphiphilic BCPs from ELA and DMLA via Cu(II)-mediated radical photopolymerization using a one-pot polymerization approach, (b) BCP1 micelles self-assemble in water at 25 °C, (c) BCP2 vesicles self-assemble when the copolymer is injected into water at 25 °C but BCP2 worm-like micelles self-assemble when the injection is carried out at 80 °C. The worm-like micelles transform into vesicles after some days at 25 °C. Cryo-transmission electron microscopy (cryo-TEM) images for (d) BCP1 self-assembled in water by direct dissolution and (e) BCP2 self-assembled by fast injection of the copolymer (dissolved in THF) into water at 25 °C. (f) Cryo-TEM images recorded 30 min after self-assembly of BCP2 by fast injection of the copolymer (dissolved in THF) into hot water (80 °C) (left image) and after 7 days at 25 °C (right spectrum). Scale bars are 100 nm.

conversion (conv. > 99%) and delivered a well-defined polymer (M_w/M_n = 1.26) (Figure S11).

Next, the living character of the photoinitiated radical polymerization of DMLA in DMSO was investigated in detail via kinetic analysis. As can be seen in Figure 1a (left panel), more than 90% of DMLA conversion was reached within 120 min including an initial induction period of 30 min. Following this induction period, kinetic analysis revealed a linear increase of the $\ln([M]_0/[M])$−time plot, which is in agreement with a constant number of propagating chains throughout the polymerization.

Moreover, GPC analysis at different polymerization times clearly illustrated the linear increase of molar mass with theoretical values and symmetrical unimodal GPC traces (M_w/M_n = 1.35−1.12) throughout the polymerization process (right panel).

Under identical conditions, the polymerization was conducted at different M/I ranging from 25 to 400 (Figures 1b and S12). The results are summarized in Table S1. In all cases, these experiments proceeded up to high monomer conversion (>95%), which is along the lines of the Green Chemistry principles. GPC analysis revealed increasing molecular weights when targeting higher DPs, with narrow molecular weight distribution (M_w/M_n = 1.19−1.26). Moreover, good agreement between M_n^{th} and M_n^{GPC} was maintained up to approximately 75 000 g·mol^{-1}. As expected, the resulting PDMLA homopolymers were glassy ($T_g \approx 65$ °C) and water-soluble at room temperature (Figure S13). Importantly, PDMLA polymers exhibited a significant chiral amplification ($[\alpha]_D^{25}$ = +25.7 for M_n = 10 000 and $[\alpha]_D^{25}$ = +28.5 for M_n = 74 000) compared to the corresponding monomer ($[\alpha]_D^{25}$ = +8.0). This kind of increase suggests that the optical activity of the polymer not only arises because of the configurational chirality in the side chain but also from a conformational chirality, most likely a secondary helical arrangement of the main chain.[51] Note that no chiral amplification was previously observed for PELA.[37]

With the hydrophilic building block in our hands, this efficient synthetic methodology was also applied to the hydrophobic and water-insoluble ELA monomer. Under strictly identical reaction conditions, a series of polymerizations were conducted in DMSO targeting DPs from 25 to 400 (Figure 1c and Table S2). Irrespective of the targeted DP, the Cu(II)-mediated photoinduced polymerizations of ELA reached almost quantitative conversions within 2 h. All the polymerizations were found to proceed under homogeneous conditions with a high degree of control (M_w/M_n = 1.19−1.24) (Figure 1c and Table S2). A representative kinetic experiment demonstrated that the photopolymerization of ELA also is fast and shows the expected features for an LRP technique (Figure S14). Note that there is no significant difference on the Cu(II)-mediated photopolymerization kinetics of ELA and DMLA monomers in comparison with a commercially available model acrylate such as methyl acrylate (compare Figures 1a, S14 and S15). The photopolymerization of ELA in its solvent precursor proceeded up to high conversion (conv. = 95%) and furnished a narrow molecular weight polymer (M_w/M_n = 1.30) (Figure S16). Finally, the excellent control over the polymerization and high chain-end functionality attained in both systems was proved by MALDI-TOF MS analysis of the lowest molar mass PDMLA and PELA samples before and after thio-bromo "click" thiotherification of bromine chain ends with thiophenol (Figure S17).[52,53] The presence of a dominant distribution with a peak-to-peak mass increment, which equals the mass of a single repeating unit, vanishing after thio-bromo "click" thiotherification of bromine

DOI: 10.1021/acssuschemeng.9b06599
ACS Sustainable Chem. Eng. 2020, 8, 1276−1284

chain ends with thiophenol, supports the high end group fidelity of the synthesized polymers. The new series of peaks emerging after the chemical modification at polymer chain ends appears 29 mass units above. This mass difference is consistent with the replacement of −Br (80) with −SPh (109) at the ω-chain ends of both polymers.

Synthesis and Thermal Properties of Amphiphilic BCPs. After demonstrating the facile preparation of well-defined homopolymers from ELA and DMLA with very different water solubilities, we pursued synthesizing amphiphilic diblock copolymers with PELA and PDMLA segments as hydrophobic and hydrophilic building blocks, respectively. In this study, we were interested to obtain BCPs able to self-assemble into various nanostructures in aqueous solution. As a proof of concept, two different PELA/PDMLA copolymers were synthesized using a one-pot polymerization approach (i.e., in situ chain extension of the first block prepared at near quantitative monomer conversion) (Figure 2a). Initially, a BCP with hydrophilic/hydrophobic ratio of 50/50 (mol/mol), named thereafter BCP1, was targeted to favor the formation of spherical micelles in water. First, the hydrophobic core block was synthesized by Cu(II)-mediated living radical photopolymerization of ELA under conditions $[ELA]_0/[EBiB]_0/[Me_6\text{-TREN}]_0/[Cu(II)Br_2]_0$ = 50/1/0.12/0.02 irradiating with UV-light (conversion 99%, M_n = 9,250, M_w/M_n = 1.23). The near-quantitative monomer conversion enabled the in situ chain extension, avoiding intermediate purification of the first block, with DMLA (DP = 50) in the second step (98% DMLA conversion) to produce PELA-*b*-PDMLA (BCP1, M_n = 18,200, M_w/M_n = 1.13).

As shown in Figure 3, the successful formation of a diblock copolymer was demonstrated by a clear shift of GPC trace toward higher molecular weights relative to the respective macroinitiator, without significant shoulders or tailing. Both blocks were grown in a controlled fashion as indicated by the close agreement between the measured M_n^{GPC} and the M_n^{th}

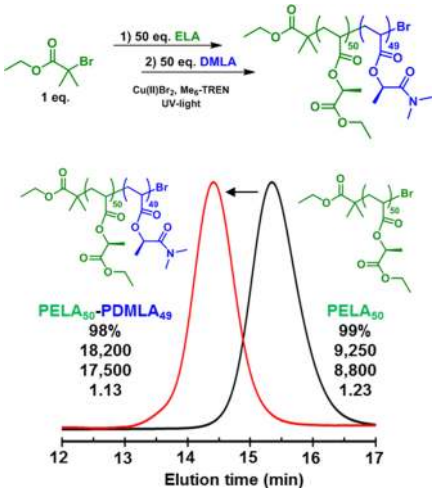

Figure 3. GPC analysis of the in situ block copolymerization via Cu(II)-mediated photopolymerization of PELA with DMLA to synthesize BCP1. Reaction conditions for the synthesis of PELA macroinitiator: $[ELA]_0/[EBiB]_0/[Me_6\text{-TREN}]_0/[Cu(II)Br_2]_0$ = 50/1/0.12/0.02 in DMSO (50 vol %) followed by the addition of deoxygenated DMLA (50 equiv) in DMSO in situ. Numbers shown together with the GPC traces correspond to monomer conversion, M_n (GPC), M_n^{th}, and M_w/M_n, respectively, from the top to the bottom.

calculated from the monomer conversions and narrow molecular weight distribution of the resulting copolymer. Note that the reverse block sequence (PDMLA−PELA) was also successful but with major discrepancy between experimental and theoretical M_n values of the resulting copolymer (Figure S18). Next, with the aim to deliver an amphiphilic BCP which could self-assemble to vesicles, the molar ratio of $[ELA]_0/[DMLA]_0$ was varied to deliver an amphiphilic diblock copolymer with a higher hydrophobic content (BCP2, Figure 2a).

In this case, a PELA macroinitiator was synthesized using a $[ELA]_0/[EBiB]_0$ = 75 under otherwise identical conditions to yield PELA with M_n = 12 640 and M_w/M_n = 1.17 which was chain-extended in situ with DMLA (DP = 25). GPC analysis after each of the two synthesis stages showed the expected growth in molar mass (Figure S19). The targeted BCPs were recovered by dialysis on a small scale against acetone (MWCO 2000) to minimize solvent waste and further analyzed by ^{1}H NMR. As an example, the analysis of BCP1 is shown in Figure S20. ^{1}H NMR analysis using a solvent such as $CDCl_3$, which is a good solvent for the PELA and PDMLA blocks, revealed the characteristic resonances of PELA (e.g., δ_8 = 5.00 ppm and δ_{10} = 4.17 ppm) and PDMLA (e.g., δ_{12} = 5.4 ppm) segments. The copolymer composition was calculated from the integrated signal of PELA CH−O group proton (δ = 5.0 ppm) with respect to the same signal of PDMLA (δ = 5.4 ppm). According to the targeted DPs, ^{1}H NMR analysis indicated a PELA/PDMLA copolymer composition of 0.51/0.49 for BCP1 and 0.80/0.20 for BCP2. Importantly, when BCP1 was dissolved in D_2O, which is a good solvent only for the PDMLA block, no precipitate was observed and only the resonances attributed to the hydrophilic PDMLA block could be detected in the ^{1}H NMR spectrum (Figure S20b), whereas those stemming from PELA cannot be detected as the block is collapsed and the solvent excluded. Overall, these observations are consistent with the formation of self-assembled structures of BCP1 in water (e.g., micelles, vesicles) with an external hydrophilic PDMLA shell and an internal hydrophobic PELA portion with restricted motion. Microphase separation behavior of the synthesized copolymers in the bulk state, but with the possibility of partial mixing of the two constitutive segments, was also proved by DSC and transmission electron microscopy (TEM) (Figure S21 and the corresponding discussion).

Self-Assembly Studies of Amphiphilic BCs in Water. With two PELA/PDMLA copolymers with different compositions in-hand, their self-assembly abilities in water were first evaluated by measuring the CAC using NR as the fluorescence probe. The fluorescence quantum yield of this molecule is much higher in an apolar environment than polar. As can be seen in Figure S22, the fluorescence intensity of NR increases rapidly through a critical polymer concentration, indicating the formation of nanoaggregates of BCP1 and BCP2 with apolar pockets. The CAC determined at the onset of slope change indicated that BCP1 acts as a container for NR above a concentration of approximately 0.034 mg L^{-1}. However, BCP2 with a higher fraction of PELA hydrophobic segment promoted aggregation to a greater extent as indicated by a lower experimental CAC value (0.022 mg L^{-1}). This is in line with stronger interaction energy ($N{\cdot}\chi$) for a longer block. Some intensity could be observed below the CAC which corresponds with the existence of monomolecular micelles. The hydrodynamic size and morphologies of the self-

DOI: 10.1021/acssuschemeng.9b06599
ACS Sustainable Chem. Eng. 2020, 8, 1276−1284

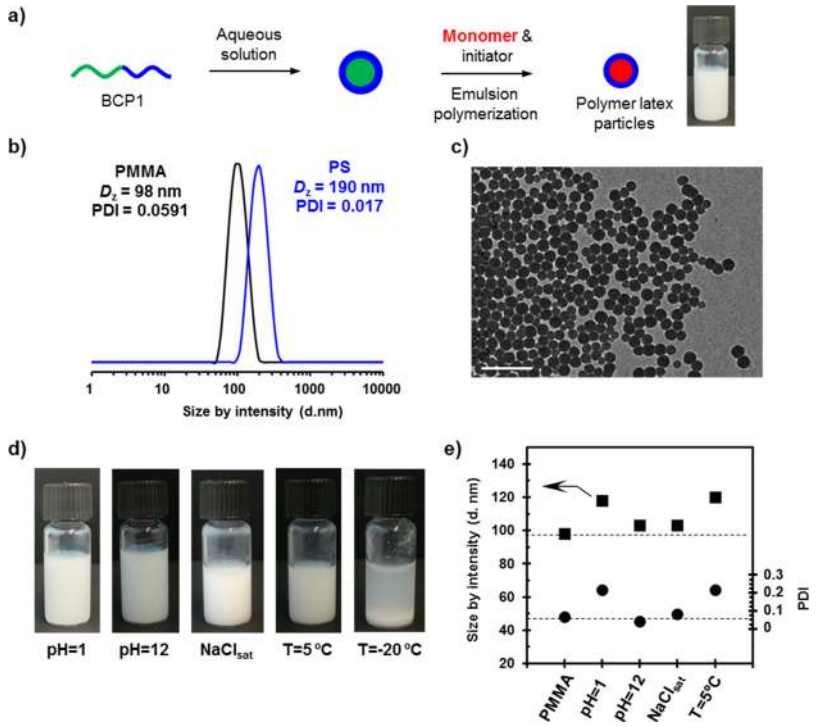

Figure 4. (a) Schematic representation of the aqueous emulsion radical polymerization of MMA and S using BCP1 as stabilizer. (b) DLS size distribution by intensity of PMMA and PS latexes stabilized by BCP1. (c) TEM image of the PMMA latex (scale bar is 100 nm). (d,e) Digital images and DLS analysis of PMMA latex under various storage conditions.

assembled structures was further investigated by dynamic light scattering (DLS) and cryo-TEM. BCP1 was added to water in a concentration above the CAC (0.5 mg mL^{-1}). A slightly turbid solution was obtained, indicating the formation of aggregates in solution (Figure S23). BCP1 consists of two blocks with identical DP. However, whereas the hydrophobic block (ELA) is collapsed in water, the hydrophilic block (DMLA) is fully expanded. Thus, low packing parameters (conical shape) corresponding to micelles were expected. DLS analysis revealed an average size of 78 nm with a dispersity of 0.224 for the nanoparticles (Figure S24a). However, the size of these particles was larger than one should expect for single spherical micelles of BCP1. The hydrophobic part of BCP1 has only DP = 50 and its contour length is smaller than half the diameter of the aggregates. The larger size could result from further aggregation of single spherical micelles because of the existence of secondary interactions, bridging, between the hydrophilic swollen micellar coronas,[54] leading to large compound micelles (LCMs) (Figure 2b). Such attractive interactions may be supported by hydrogen bonding and dipole−dipole. The cryo-TEM analysis confirmed the presence a large number of clustered particles of about 80 nm size (Figures 2d and S25), in agreement with the DLS measurement. The nonuniformity of the clusters confirms that they could not be simple micelles. The higher hydrophobic character of BCP2 required a modified approach to study its self-assembly in water. A dilute solution of BCP2 in THF (5 mg mL^{-1}) was injected into water at room temperature (final concentration of 0.5 mg mL^{-1}) (Figure 2c, right). In this case, a cloudy suspension was obtained, indicating the formation of larger aggregates in water (Figure S23) that strongly scatter light. Accordingly, DLS measurements showed a narrow size distribution centered at 148 nm (Figure S24b). The self-assembly of amphiphilic BCP2 was visualized with cryo-TEM (Figure 2e). The majority of the particles were unilamelar vesicles with a diameter of 50−150 nm. The clear contrast between the dark periphery and the hollow center indicates that these spheres are vesicular. Vesicles with higher lamellarity cannot be excluded by the injection method but were found in minimal proportion.

The differences in lyothropic assembly between BCP1 and BCP2 are in agreement with their molecular structure. In BCP2, the ratio of hydrophobic to hydrophilic block is increased, thus bilayer type of assembly that closed into vesicles is expected.[55] TEM image shown in Figure S26 was used to evaluate the membrane thickness, which statistically yields a thickness of 19 ± 0.9 nm. Interestingly, a different morphology was obtained when injecting the organic solution of the copolymer into hot water (80 °C) and cooling down to room temperature (Figure 2c, left). The assembly temperature is selected to be higher than the highest T_g of each block as observed in the thermal analysis by DSC (Figure S21). In this case, the cryo-TEM grid was prepared 30 min after sample preparation, thus giving short time for structure evolution. Cryo-TEM revealed aggregates consistent with the formation of worm-like micelles, which were obtained with a diameter of approximately 18 nm (Figure 2f left and Figure S27). This diameter is in agreement with the thickness of the membrane in the unilamellar vesicle. The formation of cylindrical micelles on BCP2 when injection was carried out at high temperature can be explained by a higher swelling of the hydrophilic block. The larger hydrophilic volume causes the ratio of hydrophilic interfacial area to become larger than the cross section of the hydrophobic block, shifting the packing parameter to the range of worm-like micelles at 80 °C. Because of the high molecular weight and low mobility of the chains in the aggregate, the worm-like micelles did not evolve to vesicles after 30 min at 25 °C. But is this system dynamic enough to observe a phase

DOI: 10.1021/acssuschemeng.9b06599
ACS Sustainable Chem. Eng. 2020, 8, 1276−1284

transition between lyotropic phases? To prove the dynamic self-assembly behavior of the system, the same sample was analyzed again after 7 days at room temperature (Figure 2f, right). After this time, cryo-TEM imaging showed unilamellar (yellow circle) and onion-like vesicles (green circle) but no cylindrical micelles could be found. Hence, we observed an interesting phase transition from cylindrical micelles to unilamellar vesicles as, after some days, the hydrophilic block size and consequently packing parameter goes back to what it is when the injection is done at room temperature. Overall, these results demonstrate that PELA/PDMLA amphiphilic copolymer can self-assemble into different morphologies such as LCMs, worm-like micelles, and unilamellar or onion-like vesicles, depending on the relative block length of the constitutive homopolymers and the preparation method of the self-assemblies.

PELA/PDMLA Amphiphilic BCPs as Stabilizers in Emulsion Polymerization. Aqueous emulsion radical polymerization processes are industrially relevant in large-scale synthesis of vinyl polymers.[56,57] A basic emulsion polymerization system involves the use of a monomer or a mixture of monomers, typically in water and in the presence of a surface active agent (surfactant). Commonly, low molecular, short-chain stabilizers are used. However, the use of amphiphilic BCP surfactants impart several advantages to the properties of the resulting emulsion because they exhibit unique properties in aqueous solution owing their low CAC and low diffusion coefficient compared to those of conventional low-molecular-weight surfactants.[58,59]

As a proof of concept test procedure, the emulsion polymerizations of MMA and S were investigated using 1.0 wt % of either BCP1 or BCP2 as macromolecular stabilizer with respect to the monomer (Figure 4a). Both reactions were performed at a monomer content of 6 wt % using potassium persulfate as an initiator at 75 °C. Under these conditions, no stable latexes were obtained using BCP2 as a macromolecular surfactant. However, BCP1 was found to be an efficient stabilizer for both commodity monomers because no coagulum was observed during the polymerization process up to high conversion. DLS analysis revealed the formation of well-defined PS and PMMA nanoparticles according to low PDI values although the average diameter for PS particles was larger (190 vs 98 nm) (Figure 4b). As can be seen in Figure S28, the smaller particle size distribution after polymerization than the initial droplet-size distribution is consistent with a predominant emulsion polymerization mechanism. Uniform and spherical latex particles were visualized by TEM (Figures 4c and S29). Both PS and PMMA latex particles stabilized with BCP1 remained stable for at least 30 days at room temperature. The stability of the PMMA latex particles was investigated under various conditions (Figure 4d,e). The nonionic nature of the BCP1 endowed excellent pH stability to the system. PMMA latex was stable when the pH was increased to 14. When the pH of the system was decreased to 1, no coagulation took place and DLS analysis after 24 h revealed only a slight increase on diameter and PDI. A similar behavior was observed after storing the PMMA suspension for 24 h in the fridge (5 °C). However, it broke after cooling at −20 °C for 24 h and thawed at room temperature (Figure 4d, right image). A promising stability to electrolyte addition was also demonstrated as PMMA latex stabilized by BCP1 was stable even after increasing the NaCl concentration until saturation.

CONCLUSIONS

In conclusion, our study demonstrates that environmentally friendly solvents can be upgraded to functional amphiphilic BCPs, suitable for applications as surfactants in nanofabrication. Efficient and sustainable functionalization of EL and DMLA green solvents with acrylate moieties generated monomers well-behaved under Cu(II)-mediated photoinduced LRP to deliver narrow and high-end functional homopolymers at near-quantitative monomer conversion. Most importantly, the EL-based polymer is hydrophobic and water-insoluble but switching the ethyl ester moiety to an *N*,*N*-dimethyl substituted amide resulted in a water-soluble vinylic polymer (PDMLA). Thus, we focused our attention on the preparation of well-defined amphiphilic diblock copolymers, combining both building blocks in one material. Several green chemistry principles apply to this approach: (i) monomer synthesis is conducted using minimal energy in a biomass-derived solvent such as Me-THF avoiding chromatographic purification, (ii) photoinduced Cu(II)-catalyzed polymerizations, conducted under mild conditions using a simple reaction setup, offer near-quantitative monomer conversions that enable block copolymerization with no intermediate purification of the first block, (iii) polymer purification protocols involves dialysis on a small scale to minimize solvent waste. The synthesized copolymers could self-assemble in water to generate nanoaggregates with different morphologies such as LCMs, worm-like micelles, and vesicles. In this regard, they exhibited efficient performance as nonionic surfactants in the preparation of well-defined PMMA and PS latexes via aqueous emulsion polymerization, demonstrating their practical significance for technological applications.

ASSOCIATED CONTENT

Supporting Information

The Supporting Information is available free of charge at https://pubs.acs.org/doi/10.1021/acssuschemeng.9b06599.

Materials and methods, additional experimental procedures, structural characterization of monomers, and additional characterization results of homopolymers and BCPs including MALDI-TOF MS spectra, kinetic plots, GPC and DLS curves, DSC and TGA traces, and TEM and cryo-TEM images (PDF)

AUTHOR INFORMATION

Corresponding Authors

*E-mail: percec@sas.upenn.edu (V.P.).
*E-mail: rodriguez@dwi.rwth-aachen.de (C.R.-E.).
*E-mail: gerard.lligadas@urv.cat (G.L.).

ORCID

Khosrow Rahimi: 0000-0002-1865-0808
Marina Galià: 0000-0002-4359-4510
Virgil Percec: 0000-0001-5926-0489
Cesar Rodriguez-Emmenegger: 0000-0003-0745-0840
Gerard Lligadas: 0000-0002-8519-1840

Author Contributions

⊥N.B. and A.M. contributed equally to this work.

Notes

The authors declare no competing financial interest.

DOI: 10.1021/acssuschemeng.9b06599
ACS Sustainable Chem. Eng. 2020, 8, 1276−1284

■ ACKNOWLEDGMENTS

This work was supported by the Spanish Ministerio de Ciencia, Innovación y Universidades through project MAT2017-82669-R (to G.L. and J.C.R.) and FPI grant BES-2015-072662 (to A.M.), the Serra Hunter Programme of the Government of Catalonia (to G.L.) and University Rovira i Virgili (DL003536 grant to N.B.). Financial support from the National Science Foundation Grants DMR-1066116, DMR-1807127 and the P. Roy Vagelos Chair at the University of Pennsylvania (to V.P.) is gratefully acknowledged. CR-E acknowledges funding by the European Commission within a H2020-NMBP-TR-IND-2018, EVPRO grant 814495-2. Dr J. Ramos (IQOXE Emulsiones Poliméricas) is thanked for sharing his expertise in polymer latexes analysis.

■ REFERENCES

(1) Bozell, J. J.; Petersen, G. R. Technology Development for the Production of Biobased Products from Biorefinery Carbohydrates-the US Department of Energy's "Top 10" Revisited. *Green Chem.* **2010**, *12*, 539−554.

(2) Gunukula, S.; Pendse, H. P.; DeSisto, W. J.; Wheeler, M. C. Heuristics To Guide the Development of Sustainable, Biomass-Derived, Platform Chemical Derivatives. *ACS Sustainable Chem. Eng.* **2018**, *6*, 5533−5539.

(3) Rinaldi, R.; Jastrzebski, R.; Clough, M. T.; Ralph, J.; Kennema, M.; Bruijnincx, P. C. A.; Weckhuysen, B. M. Paving the Way for Lignin Valorisation: Recent Advances in Bioengineering, Biorefining and Catalysis. *Angew. Chem., Int. Ed.* **2016**, *55*, 8164−8215.

(4) Isikgor, F. H.; Becer, C. R. Lignocellulosic Biomass: a Sustainable Platform for the Production of Bio-Based Chemicals and Polymers. *Polym. Chem.* **2015**, *6*, 4497−4559.

(5) Wang, Y.; Deng, W.; Wang, B.; Zhang, Q.; Wan, X.; Tang, Z.; Wang, Y.; Zhu, C.; Cao, Z.; Wang, G.; Wan, H. Chemical Synthesis of Lactic Acid from Cellulose Catalysed by Lead(II) Ions in Water. *Nat. Commun.* **2013**, *4*, 2141.

(6) Cubas-Cano, E.; González-Fernández, C.; Ballesteros, M.; Tomás-Pejó, E. Biotechnological Advances in Lactic Acid Production by Lactic Acid Bacteria: Lignocellulose as Novel Substrate. *Biofuels, Bioprod. Biorefin.* **2018**, *12*, 290−303.

(7) Dusselier, M.; Van Wouwe, P.; Dewaele, A.; Makshina, E.; Sels, B. F. Lactic Acid as a Platform Chemical in the Biobased Economy: the Role of Chemocatalysis. *Energy Environ. Sci.* **2013**, *6*, 1415−1442.

(8) Mäki-Arvela, P.; Simakova, I. L.; Salmi, T.; Murzin, D. Y. Production of Lactic Acid/Lactates from Biomass and Their Catalytic Transformations to Commodities. *Chem. Rev.* **2014**, *114*, 1909−1971.

(9) Chen, G.-Q.; Patel, M. K. Plastics Derived from Biological Sources: Present and Future: a Technical and Environmental Review. *Chem. Rev.* **2012**, *112*, 2082−2099.

(10) Yee, G. M.; Hillmyer, M. A.; Tonks, I. A. Bioderived Acrylates from Alkyl Lactates via Pd-Catalyzed Hydroesterification. *ACS Sustainable Chem. Eng.* **2018**, *6*, 9579−9584.

(11) Galaster EL 98.5 FCC, Galasolv 003, PURASOLV ELECT, and VertecBio EL are examples of commercial ethyl lactate solvents produced by Galactic, Corbion, or Vertec Biosolvents.

(12) *N,N*-Dimethyl lactamide solvent is marketed by BASF under the product name AGNIQUE AMD 3L.

(13) Pereira, C. S. M.; Silva, V. M. T. M.; Rodrigues, A. E. Ethyl Lactate as a Solvent: Properties, Applications and Production Processes − a Review. *Green Chem.* **2011**, *13*, 2658−2671.

(14) Paul, S.; Pradhan, K.; Das, A. R. Ethyl Lactate as a Green Solvent: a Promising Bio-compatible Media for Organic Synthesis. *Curr. Green Chem.* **2016**, *3*, 111−118.

(15) European Chemicals Agency. https://www-echa-europa-eu.sabidi.urv.cat/web/guest/substance-information/-/substanceinfo/100.132.568 (accessed Oct 31, 2019).

(16) *Material Safety Data Sheet MSDS AGNIQUEAMD 3L*; BASF SE: 67056 Ludwigshafen, Germany, (accessed Oct 31, 2019).

(17) Planer, S.; Jana, A.; Grela, K. Ethyl Lactate: A Green Solvent for Olefin Metathesis. *ChemSusChem* **2019**, *12*, 4655−4661.

(18) Dandia, A.; Jain, A. K.; Laxkar, A. K. Ethyl Lactate as a Promising Bio Based Green Solvent for the Synthesis of Spiro-Oxindole Derivatives via 1,3-Dipolar Cycloaddition Reaction. *Tetrahedron Lett.* **2013**, *54*, 3929−3932.

(19) Bertrand, O.; Wilson, P.; Burns, J. A.; Bell, G. A.; Haddleton, D. M. Cu(0)-Mediated Living Radical Polymerisation in Dimethyl Lactamide (DML); an Unusual Green Solvent with Limited Environmental Impact. *Polym. Chem.* **2015**, *6*, 8319−8324.

(20) Moreno, A.; Garcia, D.; Galià, M.; Ronda, J. C.; Cádiz, V.; Lligadas, G.; Percec, V. SET-LRP in the Neoteric Ethyl Lactate Alcohol. *Biomacromolecules* **2017**, *18*, 3447−3456.

(21) Lligadas, G.; Grama, S.; Percec, V. Single-Electron Transfer Living Radical Polymerization Platform to Practice, Develop and Invent. *Biomacromolecules* **2017**, *18*, 2981−3008.

(22) Zhang, N.; Samanta, S. R.; Rosen, B. M.; Percec, V. Single Electron Transfer in Radical Ion and Radical-Mediated Organic, Materials and Polymer Synthesis. *Chem. Rev.* **2014**, *114*, 5848−5958.

(23) EL is produced by the esterification reaction of ethanol and lactic acid whereas DML can be easily synthesized either from the reaction of lactic acid esters or lactide with dimethyl amine.

(24) Bell, G. A.; Tovey, I. D. Process for Producing Lactamide Compounds, New Lactamide Compounds and Formulations Containing Lactamide Compounds. WO2007107745A2, Sep 27, 2007.

(25) Henneberry, M.; Snively, J.; Vasek, G.; Datta, R. Biosolvent Composition of Lactate Ester and D-Limonene with Improved Cleaning and Solvating Properties. U.S. Patent 2,003,0171 A1, Sep 11, 2003.

(26) Gronwald, O.; Weber, M. AGNIQUE AMD 3L as Green Solvent for Polyethersulfone Ultrafiltration Membrane Preparation. *J. Appl. Polym. Sci.* **2019**, *137*, 48419.

(27) Sobieski, R. T. Aqueous Compositions Comprising Esters of Lactic Acid and Methods of Use.WO2005049719A2, June 2, 2005.

(28) Nikles, S. M.; Piao, M.; Lane, A. M.; Nikles, D. E. Ethyl Lactate: a Green Solvent for Magnetic Tape Coating. *Green Chem.* **2001**, *3*, 109−113.

(29) Sen, R.; Sivarajan, R.; Rueckes, T.; Segal, B. M. Applicator Liquid Containing Ethyl Lactate for Preparation of Nanotube Films. WO2006007206A3, Jan 19, 2006.

(30) Llevot, A.; Dannecker, P.-K.; von Czapiewski, M.; Over, L. C.; Söyler, Z.; Meier, M. A. R. Renewability is not Enough: Recent Advances in the Sustainable Synthesis of Biomass-Derived Monomers and Polymers. *Chem.—Eur. J.* **2016**, *22*, 11510−11521.

(31) Zhu, Y.; Romain, C.; Williams, C. K. Sustainable Polymers from Renewable Resources. *Nature* **2016**, *540*, 354−362.

(32) Schneiderman, D. K.; Hillmyer, M. A. 50th Anniversary Perspective: There is a Great Future in Sustainable Polymers. *Macromolecules* **2017**, *50*, 3733−3749.

(33) Purushothaman, M.; Krishnan, P. S. G.; Nayak, S. K. Poly(alkyl lactate acrylate)s Having Tunable Hydrophilicity. *J. Appl. Polym. Sci.* **2014**, *131*, 40962.

(34) Purushothaman, M.; Krishnan, P. S. G.; Nayak, S. K. Tunable Hydrophilicity of Poly(ethyl lactate acrylate-*co*-acrylic acid). *J. Renewable Mater.* **2015**, *3*, 292−301.

(35) Purushothaman, M.; Gopala Krishnan, P. S.; Nayak, S. K. Effect of Isoalkyl Lactates as Pendant Group on Poly(acrylic acid). *J. Macromol. Sci., Part A: Pure Appl.Chem.* **2014**, *51*, 470−480.

(36) Purushothaman, M.; Krishnan, P. S. G.; Nayak, S. K. Effect of Nano Sepiolite Fiber on the Properties of Poly(ethyl lactate acrylate): Hydrophilicity and Thermal Stability. *Mater. Focus* **2018**, *7*, 101−107.

(37) Bensabeh, N.; Moreno, A.; Roig, A.; Monaghan, O. R.; Ronda, J. C.; Cádiz, V.; Galià, M.; Howdle, S. M.; Lligadas, G.; Percec, V. Polyacrylates Derived from Biobased Ethyl Lactate Solvent via SET-LRP. *Biomacromolecules* **2019**, *20*, 2135−2147.

(38) Moreno, A.; Bensabeh, N.; Parve, J.; Ronda, J. C.; Cádiz, V.; Galià, M.; Vares, L.; Lligadas, G.; Percec, V. SET-LRP of Bio- and

DOI: 10.1021/acssuschemeng.9b06599
ACS Sustainable Chem. Eng. 2020, 8, 1276−1284

Petroleum-Sourced Methacrylates in Aqueous Alcoholic Mixtures. *Biomacromolecules* **2019**, *20*, 1816−1827.
(39) Reynolds, D. D.; Kenyon, W. O. Acrylic Ester-Amides and Polymers Thereof. U.S. Patent 2,458,420 A, Jan 4, 1949.
(40) Holmberg, A. L.; Reno, K. H.; Wool, R. P.; Epps, T. H., III Biobased Building Blocks for the Rational Design of Renewable Block Polymers. *Soft Matter* **2014**, *10*, 7405−7424.
(41) Brown, H. R.; Krappe, U.; Stadler, R. Effect of ABC Triblock Copolymers with an Elastomeric Midblock on the Adhesion between Immiscible Polymers. *Macromolecules* **1996**, *29*, 6582−6588.
(42) Ruzette, A.-V.; Leibler, L. Block Copolymers in Tomorrow's Plastics. *Nat. Mater.* **2005**, *4*, 19−31.
(43) Sainz, M. F.; Souto, J. A.; Regentova, D.; Johansson, M. K. G.; Timhagen, S. T.; Irvine, D. J.; Buijsen, P.; Koning, C. E.; Stockman, R. A.; Howdle, S. M. A Facile and Green Route to Terpene Derived Acrylate and Methacrylate Monomers and Simple Free Radical Polymerisation to Yield New Renewable Polymers and Coatings. *Polym. Chem.* **2016**, *7*, 2882−2887.
(44) Anastasaki, A.; Nikolaou, V.; Zhang, Q.; Burns, J.; Samanta, S. R.; Waldron, C.; Haddleton, A. J.; McHale, R.; Fox, D.; Percec, V.; Wilson, P.; Haddleton, D. M. Copper(II)/Tertiary Amine Synergy in Photoinduced Living Radical Polymerization: Accelerated Synthesis of ω-Functional and α,ω-Heterofunctional Poly(acrylates). *J. Am. Chem. Soc.* **2014**, *136*, 1141−1149.
(45) Jones, G. R.; Whitfield, R.; Anastasaki, A.; Haddleton, D. M. Aqueous Copper(II) Photoinduced Polymerization of Acrylates: Low Copper Concentration and the Importance of Sodium Halide Salts. *J. Am. Chem. Soc.* **2016**, *138*, 7346−7352.
(46) Anastasaki, A.; Nikolaou, V.; Nurumbetov, G.; Truong, N. P.; Pappas, G. S.; Engelis, N. G.; Quinn, J. F.; Whittaker, M. R.; Davis, T. P.; Haddleton, D. M. Synthesis of Well-Defined Poly(acrylates) in Ionic Liquids via Copper(II)-Mediated Photoinduced Living Radical Polymerization. *Macromolecules* **2015**, *48*, 5140−5147.
(47) Laun, J.; Vorobii, M.; de los Santos Pereira, A.; Pop-Georgievski, O.; Trouillet, V.; Welle, A.; Barner-Kowollik, C.; Rodriguez-Emmenegger, C.; Junkers, T. Surface Grafting via Photo-Induced Copper-Mediated Radical Polymerization at Extremely Low Catalyst Concentrations. *Macromol. Rapid Commun.* **2015**, *36*, 1681−1686.
(48) Vorobii, M.; de los Santos Pereira, A.; Pop-Georgievski, O.; Kostina, N. Y.; Rodriguez-Emmenegger, C.; Percec, V. Synthesis of Non-fouling Poly[N-(2-hydroxypropyl)methacrylamide] Brushes by Photoinduced SET-LRP. *Polym. Chem.* **2015**, *6*, 4210−4220.
(49) Vandenbergh, J.; Reekmans, G.; Adriaensens, P.; Junkers, T. Synthesis of Sequence-Defined Acrylate Oligomers via Photo-induced Copper-mediated Radical Monomer Insertions. *Chem. Sci.* **2015**, *6*, 5753−5761.
(50) Martí, M.; Molina, L.; Alemán, C.; Armelin, E. Novel Epoxy Coating Based on DMSO as a Green Solvent, Reducing Drasticallythe Volatile Organic Compound Content and Using Conducting Polymers As a Nontoxic Anticorrosive Pigment. *ACS Sustainable Chem. Eng.* **2013**, *1*, 1609−1618.
(51) Bauri, K.; De, P.; Shah, P. N.; Li, R.; Faust, R. Polyisobutylene-Based Helical Block Copolymers with pH-Responsive Cationic Side-Chain Amino Acid Moieties by Tandem Living Polymerizations. *Macromolecules* **2013**, *46*, 5861−5870.
(52) Rosen, B. M.; Lligadas, G.; Hahn, C.; Percec, V. Synthesis of Dendritic Macromolecules through Divergent Iterative Thio-Bromo "Click" Chemistry and SET-LRP. *J. Polym. Sci., Part A: Polym. Chem.* **2009**, *47*, 3940−3948.
(53) Rosen, B. M.; Lligadas, G.; Hahn, C.; Percec, V. Synthesis of Dendrimers Through Divergent Iterative Thio-Bromo "Click" Chemistry. *J. Polym. Sci., Part A: Polym. Chem.* **2009**, *47*, 3931−3939.
(54) Israelachvili, J. N. *Intermolecular and Surface Forces*, 2nd ed.; Academic Press: London, U.K., 1992.
(55) Smart, T.; Lomas, H.; Massignani, M.; Flores-Merino, M. V.; Perez, L. R.; Battaglia, G. Block Copolymer Nanostructures. *Nano Today* **2008**, *3*, 38−46.
(56) Asua, J. M. Emulsion Polymerization: From Fundamental Mechanisms to Process Developments. *J. Polym. Sci., Part A: Polym. Chem.* **2004**, *42*, 1025−1041.
(57) Rigoussen, A.; Verge, P.; Raquez, J. M.; Dubois, P. *Chemistry and Technology of Emulsion Polymerisation*; John Wiley & Sons Ltd: Oxford, U.K., 2013; Vol. *6*.
(58) Raffa, P.; Wever, D. A. Z.; Picchioni, F.; Broekhuis, A. A. Polymeric Surfactants: Synthesis, Properties, and Links to Applications. *Chem. Rev.* **2015**, *115*, 8504−8563.
(59) George, S.; Champagne-Hartley, R.; Deeter, G. A.; Campbell, J. D.; Reck, B.; Urban, D.; Cunningham, M. F. Amphiphilic Block Copolymers as Stabilizers in Emulsion Polymerization: Effects of the Stabilizing Block Molecular Weight Dispersity on Stabilization Performance. *Macromolecules* **2015**, *48*, 8913−8920.

DOI: 10.1021/acssuschemeng.9b06599
ACS Sustainable Chem. Eng. 2020, 8, 1276−1284